Journal of
APPLIED PACKAGING RESEARCH

RESEARCH ARTICLE

# Application of Computational MBD for Simulation of Wrap Packaging Performance

**Niels Hojen Ostergaard***
Rhine-Waal University of Applied Sciences

**Stephane Danjou**
Rhine-Waal University of Applied Sciences

## ABSTRACT

*This paper concerns evaluation of the performance of plastic wrap films applied for packaging engineering by numerical simulation. In particular, the feasibility of computational techniques as supporting tool for packaging testing is investigated. A wrap film model constituted by a web of point masses connected by springs and dampers is applied to a number of stacked box-shaped objects. These will be modeled as perfectly rigid using simulation techniques from 3D multibody dynamics. Contact mechanics are simulated by penalization methods. A simple example demonstrates the potential of the developed framework.*

## KEY WORDS

*multibody dynamics, packaging testing, numerical simulation*

***Niels Hojen Ostergaard**
*Corresponding Author*
niels.ostergaard@hochschule-rhein-waal.de

## INTRODUCTION

Application of plastic wrap films is among the most common techniques in packaging engineering applied to ensure that objects are firmly restrained from moving during transportation. While various techniques for obtaining a suitable plastic wrap of objects (stretching, shrinking etc.) are widely applied in the industry, surprisingly little research is available on theoretical methods for performance prediction. An overview of common faults and failures related to plastic wrap film packaging is presented by Singh et al. [1].

However, various experimental methods have been developed to evaluate the performance of packaging wraps subjected to static or dynamic loads, see for example Singh et al. [2]. A common test method is to place a stack of packed objects on a plane, which is rotated in order to evaluate how large the slips occurring between the packed objects below the packaging film are. This test principle is illustrated in Figure 1 in which a stretch wrap is visualised as a blue web above a stack of green boxes packed on a pallet.

The theory and simulation models summarized in this paper are considered to be of general interest for packaging engineering professionals. The objective of the present paper is to investigate the feasibility of application of techniques from computational multibody dynamics (MBD) for evaluation of wrap performance as supporting tool for experimental packaging testing. A parametric MBD model of the dynamic behaviour of a number of unconstrained stacked objects will be developed based on the computational formulations of the 3D Newton-Euler equations for dynamic equilibrium developed by Nikravesh [3] and contact mechanics developed by Goyal et al. [4]. A similar approach was shown by the authors to function well for simulation of plane bottle conveyor systems [5]. Additionally, a packaging film will be simulated by methods from cloth modelling, see [6], as a web of point masses connected by springs and dampers. In the present paper, only boxed-shaped objects wrapped with a linear elastic packaging film will be considered. The presented method is however capable of representing objects of arbitrary shape and furthermore to account for the highly non-linear constitutive behaviour (material law) of plastic films. Examples of how the material characteristics can be obtained experimentally were presented by Bisha [7], who developed both principles for measuring of material stiffness along with film tension and containment force along with material stiffness. Statistical analysis showed reasonable similarity between containment force and material stiffness obtained using the two developed principles. Etzmuss et al. [8] demonstrated how parameters measured for a film continuum could be related to the properties of a particle system. This was conducted by deriving the particle system properties from classical continuum mechanics by linearization, application of a local reference frame and finally finite difference discretization. The obtained results showed that the developed method due to rotational invariance was well-posed for simulation of highly deformable objects, like textiles.

In the current approach, all considered bodies will be considered rigid, since MBD techniques usually are not well-posed for simulations accounting for deformability. Since deformations between packed objects usually cause interlocking effects restraining the motions, this limitation is in most cases considered likely to lead to conservative results with respect to slip prediction. Studies in how elements similar to wrap films may be simulated as membranes using finite element techniques (FEM) were conducted by Rossi et al. [9] and Contri et al. [10]. In both cases, the developed methods were focused on derivation of procedures based on continuum mechanics for handling of the finite strain in membrane structures. However,

solution to continuum mechanics problems using FEM usually leads to a larger number of nonlinear equations to be solved in order to account for deformability than MBD, which only accounts for the motion of the centers of gravity (CoGs) of the considered objects. Therefore, MBD based simulations are more likely to be serve as basis for a tool for prediction of wrap film performance, since the developed models can be solved faster.

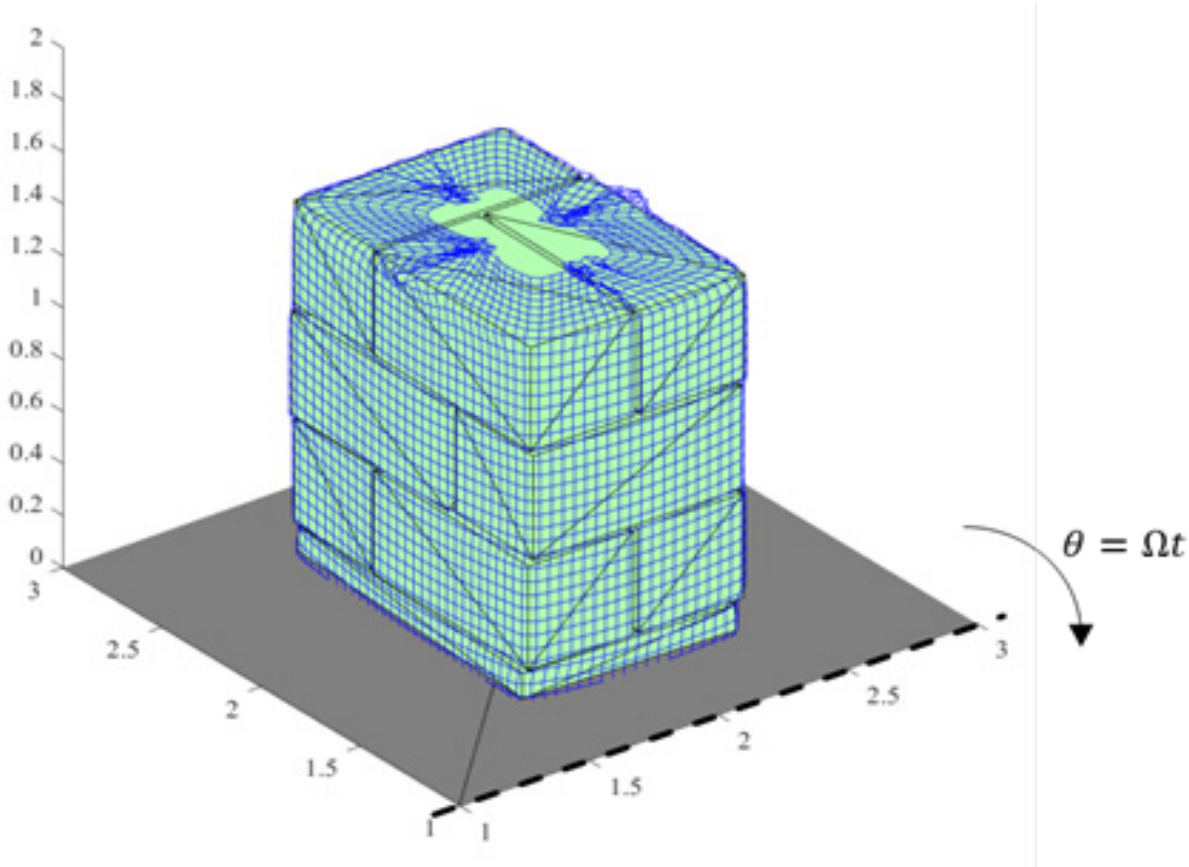


*Figure 1. Visualization of the a test principle for experimental investigation of the performance of packaging wrap films.*

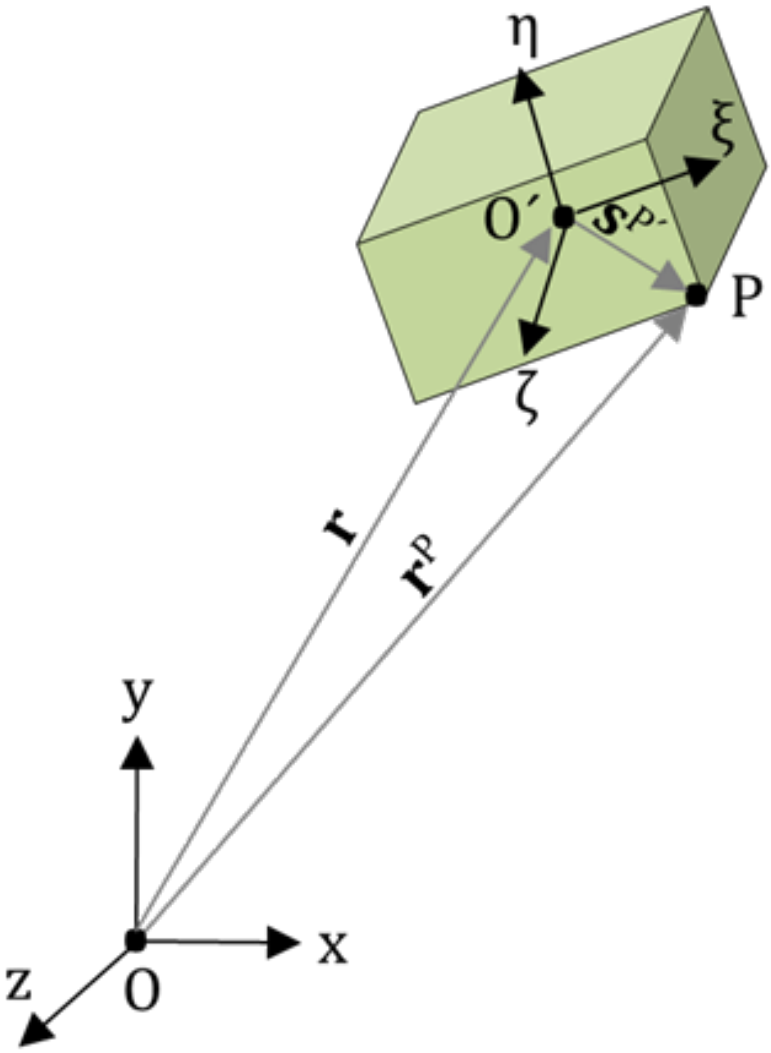


*Figure 2 Local (xyz) and global (ξηζ) coordinate frames*

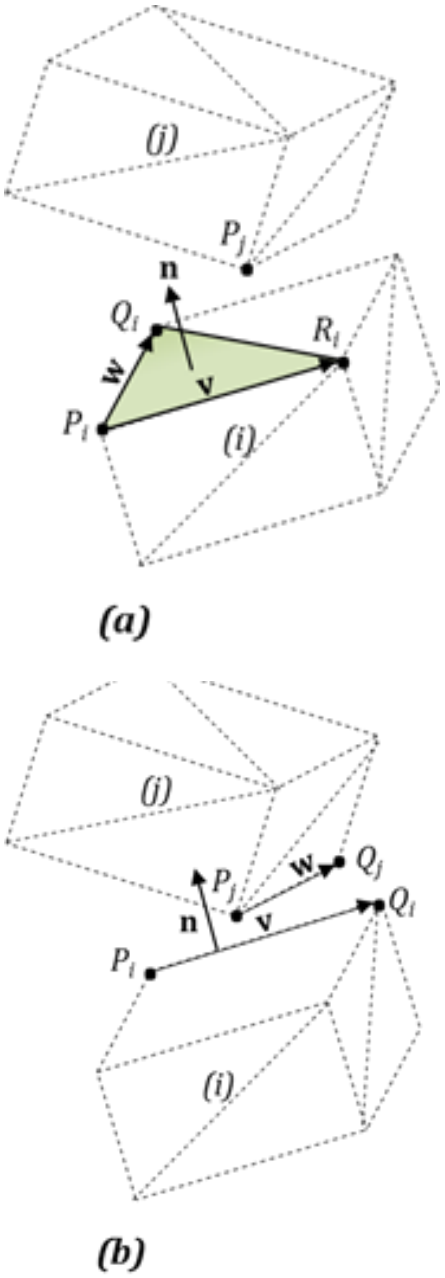


*Figure 3 (a) Point-to-Surface contact, (b) Line-to-Line contact*

## THEORY

In this section, the theoretical basis for the developed parametric simulation model is described.

### Position and spatial orientation of rigid bodies

The position of the center of gravity of each considered body in a 3D space is given by the vector **r** with three coordinates, see Figure 2. In order to describe the spatial orientation of a rigid body in a 3D space, four parameters are required. As basis for 3D rotations, the approach proposed by Nikravesh [3] will be followed, using the four Euler parameters e0 ...e3 contained in the vector **p.**

$$\mathbf{r} = \begin{pmatrix} x \\ y \\ z \end{pmatrix} \qquad \mathbf{p} = \begin{pmatrix} e_0 \\ e_1 \\ e_3 \\ e_4 \end{pmatrix} \tag{1}$$

On basis of the seven coordinates given in equation (1), the spatial geometry of a rigid body in a 3D space is fully specified. For every body considered, a local ξηζ-coordinate frame with origo in the center of gravity will be attached to each body and rotate along with it. The position of any point *P* inside the body is now given by

$$\mathbf{r}^P = \mathbf{r} + \mathbf{A}\mathbf{s}^P \tag{2}$$

where **A** is a rotation matrix and $s^{P`}$ is the position of point P in the local body frame. In general, we will let primes denote local frames. Differentiation with respect to time gives the following result

$$\dot{\mathbf{r}}^P = \dot{\mathbf{r}} + \mathbf{A}\tilde{\boldsymbol{\omega}}`\mathbf{s}^{P`} \tag{3}$$

in which $\dot{\mathbf{r}}$ denotes the velocity of the center of gravity of the considered body. The skew matrix of $\tilde{\boldsymbol{\omega}}`$ of the angular velocities $\tilde{\boldsymbol{\omega}}`$ in the local body frame in this context simply constitutes an alternative way of performing a cross-product operation and is commonly applied in MBD simulations.

In order to obtain a sequentially independent rotation procedure, Euler's rotation theorem is applied. Rotations are hereby described in terms of an angle φ and an axis described in terms of a vector **e**. The four Euler parameters are in terms of φ and **e** given by

$$e_0 = \cos\left(\frac{\varphi}{2}\right) \tag{4}$$

$$\mathbf{e} = \begin{pmatrix} e_1 \\ e_2 \\ e_3 \end{pmatrix} = \mathbf{u}\sin\left(\frac{\varphi}{2}\right) \tag{5}$$

The rotation matrix is now in accordance with Nikrawesh [1] given by

$$\mathbf{A} = (2e_0^2 - 1)\mathbf{I} + 2(\mathbf{e}^{\ T} + e_0\tilde{\mathbf{e}}) \tag{6}$$

For specified position of the center of gravity and spatial orientation of any rigid body considered, these equations allow for determination of position and velocity of any point inside the rigid body.
Since the considered motions are unconstrained, the motion properties are governed solely by their initial positions and the external forces acting on the bodies.

### Equations of motion and numerical integration

The considered rigid bodies are subject to forces due to gravity, contact and friction. The motion of the center of gravity is governed by Newton's 2nd law, which on vector form can be written

$$\mathbf{F} = m\ddot{\mathbf{r}} \tag{7}$$

$$\dot{\mathbf{r}}^{(i+1)} = \dot{\mathbf{r}}^{(i)} + \ddot{\mathbf{r}}^{(i)}\Delta t = \dot{\mathbf{r}}^{(i)} + \ddot{\mathbf{r}}^{(i)}\left(\frac{1}{m}\mathbf{F}^{(i)}\right) \tag{8}$$

$$\mathbf{r}^{(i+1)} = \mathbf{r}^{(i)} + \Delta t + \dot{\mathbf{r}}^{(i+1)}\Delta t \tag{9}$$

with time step of magnitude

$$\Delta t = t^{(i+1)} - t^{(i)}$$

It is convenient to formulate the moment equilibrium in local coordinates, since this enables application of an inertia tensor $\mathbf{J}`$ with constant entries. This is due to that the body inertia properties are constant in the local body frame, but not in global coordinates. The moment equilibrium is on vectorial form given by

$$\mathbf{M}` = \mathbf{J}`\dot{\boldsymbol{\omega}}` + \tilde{\boldsymbol{\omega}}`\mathbf{J}`\boldsymbol{\omega}` \tag{10}$$

In this equation, we may isolate the local angular acceleration and obtain the angular velocities in the body frame by numerical integration. These can be related directly to the time derivatives of the Euler-parameters by

$$\dot{\mathbf{p}} = \frac{1}{2}\mathbf{L}^{\mathrm{T}}\boldsymbol{\omega}' \tag{11}$$

where L can be obtained in terms of the Euler parameters

$$\mathbf{L} = \begin{bmatrix} -e_1 & e_0 & e_3 & -e_2 \\ -e_2 & -e_3 & e_0 & e_1 \\ -e_3 & e_2 & -e_1 & e_0 \end{bmatrix} \tag{12}$$

By numerical integration of equation (10), the Euler parameters can be calculated as representation of the spatial orientation of the body in the global coordinate frames. For prescribed forces, the position and spatial orientation can now be calculated by numerical integration of the equations of motion.

Gravitational forces are added directly to the CoG of all considered moving bodies.

Contact forces are accounted for using penalization methods as demonstrated by the authors in [5]. When using penalization based contacts, a spring and a damping force is added in each point in contact on moving bodies. In the present context, each body will be considered surrounded by a contact volume with constant thickness δ. Once contact is detected, the penetration depth determines the deflection required to set a spring force simulating contact. The corresponding damping force accounting for dissipation of energy in impacts is determined on basis of the relative velocity between the two bodies in contact. It is noted, that friction and contact forces generate moments around the CoG of the dynamic bodies, which must be calculated and added for each time step.

Friction will be applied using a simple Coulomb-law, where frictional forces are applied to bodies in contact only on basis of a dynamic frictional coefficient $\mu$ and the acting normal force (obtained from the contact penalization parameters, see section 2.3). However, in order to simulate frictional effects at low speeds, a regularization polynomial of 2nd order *p(v)* is applied in a similar fashion as in [5] and the friction force is given by

$$\mathbf{F}_{\mu} = \begin{cases} -p(v)\mu\dfrac{\mathbf{v}}{\|\mathbf{v}\|}\mathbf{N} & v \le v_{\lim} \\ -\mu\dfrac{v}{\|v\|}\mathbf{N} & v > v_{\lim} \end{cases} \tag{13}$$

With the equations in this section, the position and spatial orientation of a body can be calculated on basis of the acting forces.

**Contact detection**

In accordance with Goyal et al. [4], each body can be considered as made up by a set of surfaces, a set of lines and a set of points. On this basis, two bodies might be subjected to surface-to-surface, surface-to-line, surface-to-point, line-to-line, line-to-point or point-to-point contacts. However, it was furthermore shown, that an infinitesimal rotation of two bodies in contact, inevitably will convert any contact to a point-to-surface or a line-to-line contact. An exception, where this might not hold is contact in convex corners, which is not relevant in the present context. Contact detection will therefore only be performed for these two cases.

All bodies will be modelled as constituted by a set of triangular surfaces with a corresponding set of lines and a set of points. This approach is practical, since it in general requires less effort to approximate a surface with a set of triangles than with a set of rectangles.

In order for a point $P_j$ in the *j'th* body to be in contact with the triangular surface spanned by $P_i$, $Q_i$ and $R_i$ on the *i'th* body, the point must lie within the plane spanned by the triangle and be sufficiently close to each other for the contact layers of the two bodies to overlap, see Figure 3.a. A.S. Knudsen et al. [11] converted the formulation proposed by Goyal et al. [4] to the following equations

$$P_i + \mathbf{w}k_1 + \mathbf{v}k_2 + \mathbf{n}k_3 = P_j \tag{14}$$

In which the vectors v, w and n are given by

$$\mathbf{w} = \left|P_iQ_i\right| \quad \mathbf{v} = \left|P_iR_i\right| \quad \mathbf{n} = \frac{\mathbf{w}\times\mathbf{v}}{\left\|\mathbf{w}\times\mathbf{v}\right\|} \tag{15}$$

The contact condition can after solving the linear system in equation (14) be formulated as

$$k_1 \geq 0, k_2 \geq 0, k_1 + k_2 \leq 1, k_3 < 2\delta$$

In an equivalent fashion, it was shown in [11] that the contact point between the lines spanned by $P_i$ and $Q_i$ on the *i'th* body and the points $P_j$ and $Q_j$ on the *j'th* body, see Figure 3.b, can be determined by solving the linear system

$$P_i + \mathbf{w}k_1 + \mathbf{n}k_3 = P_j + \mathbf{v}k_2 \tag{16}$$

with vectors given by

$$\mathbf{w} = \left|P_jQ_j\right| \quad \mathbf{v} = \left|P_iQ_i\right| \quad \mathbf{n} = \frac{\mathbf{w}\times\mathbf{v}}{\left\|\mathbf{w}\times\mathbf{v}\right\|} \tag{17}$$

The contact condition is now given by

$$0 \leq k_1 \leq 1, 0 \leq k_2 \leq 1, k_3 \leq 2\delta$$

With this mathematical framework available, contact detection is performed by checking all points in a body against all surfaces in all other bodies, and all lines in a body against all lines in all other bodies.

The application of bounding boxes and a hierarchical contact detection has not been considered in the current work. While this would speed up contact detection for complex body geometries significantly, there is little or no gain for a web of point masses.

**Wrap film model**

A packaging wrap film is now modelled as a system of point masses connected by springs and dampers in a rectangular web as shown in Figure 4. The mechanics of the web is simpler than for the dynamic bodies, since the point masses possess no spatial orientation, but only have position coordinates. Contact detection between point masses and the dynamic bodies can be performed as point-to-surface contacts by solving equation (14). Once contact is detected, friction and contact forces are added in the same fashion as for the dynamic bodies. For each point mass considered, spring and damping forces are added on basis of the positions of the surrounding three point masses and the relative velocities. It is noted, that contact only can occur between point masses and surfaces and that the lines drawn between two neighboring masses therefore may penetrate the dynamic bodies. However, since the contact takes places in a narrow contact volume surrounding point masses and bodies, experience has shown that this will not happen for a sufficiently fine mesh in the web of point masses. The complex problem related to the self-contact common in computer simulation of cloth is estimated to impose very little influence on the obtained results in the considered type of packaging problems and is therefore neglected. The tensile and compressive stiffness parameters may differ, in order to simulate the low compressive stiffness of a wrap film, and the two states are connected with a regularisation similar to the one applied to the Coulomb friction in equation (13).

## NUMERICAL IMPLEMENTATION

The equations described in chapter 2 were implemented in a Mablab script. Unconstrained dynamic elements are defined as bodies, while fixed elements or elements with prescribed motion (for example a rotated plane) are defined as world elements. On basis of definition of points and surfaces for each of these two categories, points, edge lines and surfaces are calculated in local coordinates and saved for further application during contact detection. A set of initial conditions are defined along with mass and moment of inertia for each moving body. A web of point masses is defined directly by specifying the dimensions of the web and the level of stretch in terms of the undeformed length of the web springs.

As first step in the time integration loop, the position of all points in each body and web mass are calculated in global coordinates utilizing equation (2). Contact checks are performed by checking all points against all surfaces and all lines against all lines applying equations (14) and (16). The contact pairs are saved for force calculation. Contact checks are from a computational perspective the by far most costly part of the calculation. Experience has shown, that full contact detection may not be necessary for each time step, if the time discretization is sufficiently fine. For many problems, it is sufficient to detect the contact pairs, and before defining contact forces in every time step to check if the saved contact pairs have remained in contact.

Once contacts are detected, force calculation accounting for contacts, gravity, springs (in web) and friction is performed and positions and spatial orientations of all bodies are calculated by numerical integration of equations (7), (10) and (11).

A visualization of the structure of the developed simulation code is presented as flowchart in Figure 6. The numerical implementation of the equations in section 2 mainly requires functionalities such as loop structures and linear algebraic operations. Therefore, the numerical implementation could might as well have been performed in any program suited for scientific programming (for example Python). However, the easy configurable plotting functionalities in Matlab enable fast visualization of the obtained results.

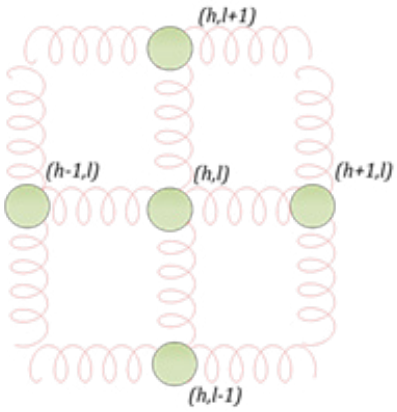


*Figure 4 Packaging wrap film modelled as a web of point masses*

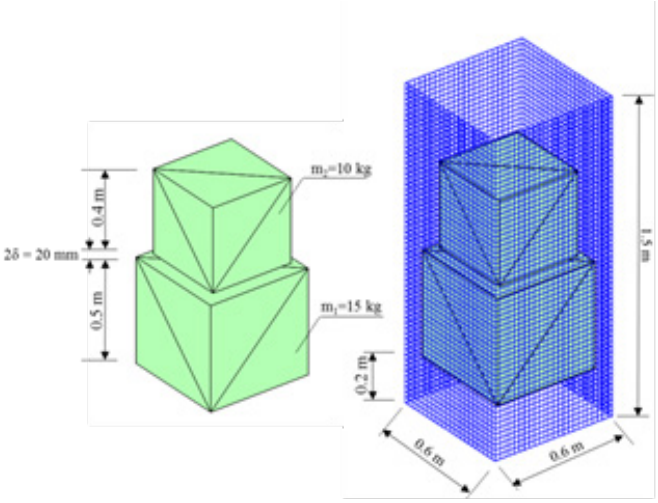


*Figure 5 Dimensions and masses of the considered two cube shaped boxes and the web simulating a wrap film*

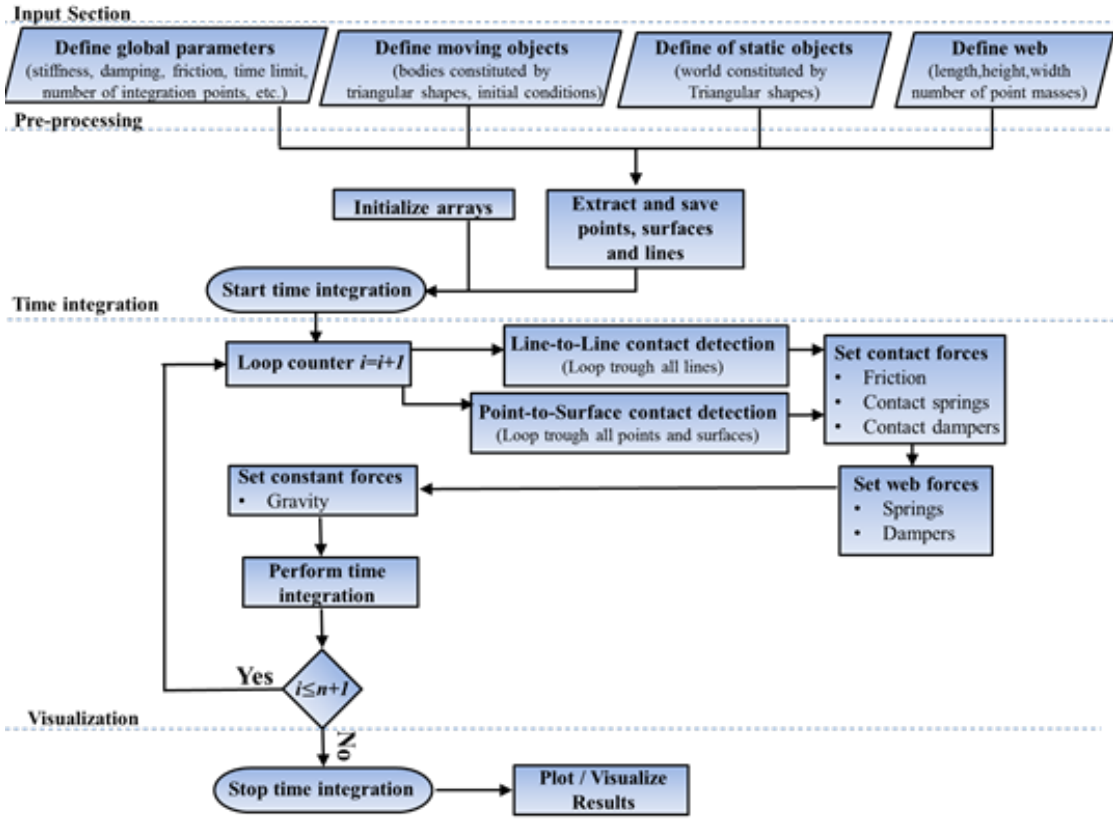


*Figure 6 Flowchart of the developed simulation code*

## RESULTS

The developed simulation tool will for the sake of simplicity be tested using a simpler geometry than shown in Figure 1. Two cube shaped boxes placed on top of each other will therefore be applied as benchmark case. A case, where the boxes are allowed to slide freely will be compared to a case where the two boxes are wrapped in a film simulated as a web of springs. The geometries, masses and contact layer thickness parameters are defined in Figure 5. The two boxes will be placed on a world surface, which for 1 second will remain static, in order for the wrap film to be applied in the case containing a such. After one second has past, a uniform angular velocity of 0.1 rad/s (5.73 deg/s) will be applied, and it will be investigated how the boxes slip. The total simulation time is set to $t=6\ s$ in 24000 steps with contact detection performed for each time step for the first 0.5 seconds in order for the wrap film to attach properly and afterwards for each fifth time step. The friction coefficient for body-to-body contact and body-to-world contact is set to $\mu=0.3$ with regularization parameter $v_{lim}=10$ mm/s in equation (13).

The body-to-body contact stiffness is set to 200000 N/m with a damping of 10 kg/s and the point-mass-to-body contact stiffness to 4000 N/m with a damping of 1 kg/s. The web spring stiffness is defined as 2000 N/m with a low level of material damping specified to 0.1 kg/s. A friction coefficient of

μ=0.9 is specified between bodies and point-masses to simulate the sticking effect commonly occurring between wrap film and packed objects. In order to investigate how well the wrap film model performs, high stretches with respect to the undeformed length are applied. The horizontal stretch is set to 40% while the vertical stretch is set to 20%. A total of 5856 point masses are applied for the web generation.

Contact stiffness and damping was along web material properties and friction partially estimated using the methods given in [4] on basis of typical values, but also to some extend determined by trial and error to demonstrate the functionality of the developed framework. Accurate values for stiffness and damping are severely dependent on the materials simulated, and cannot be assessed accurately without experimental work. In the current case, the accuracy of the contact stiffness and light damping parameters are considered of minor importance due to the non-impulse nature of the modeled contacts.

The obtained results are visualized in Figure 7 for selected angles of rotation of the plane on which the boxes are placed. As slip measure, the distance between the CoGs of the two boxes will simply be applied for the sake of simplicity. The results are shown for the last two simulated seconds in Figure 8. For the wrapped case, slippage can be observed to be prevented and eventually the simulated wrap film causes both boxes to tip over due to the dislocation of the CoG of the boxes. Finally, the distance between CoGs in the wrapped case increases beyond the level of the unwrapped case, as the top box is released from the film the falls of the rotated plane. The velocities obtained from the simulations are shown in Figure 9. For the unwrapped case, motions can be observed to be prevented until the theoretical slip limit $\mu=atan(\theta)$ obtained using Newton's 2nd law is exceeded. The velocities in the wrapped case can be observed to be larger than for the unwrapped. This effect occurs as both boxes tip over and fall onto the rotated plane.

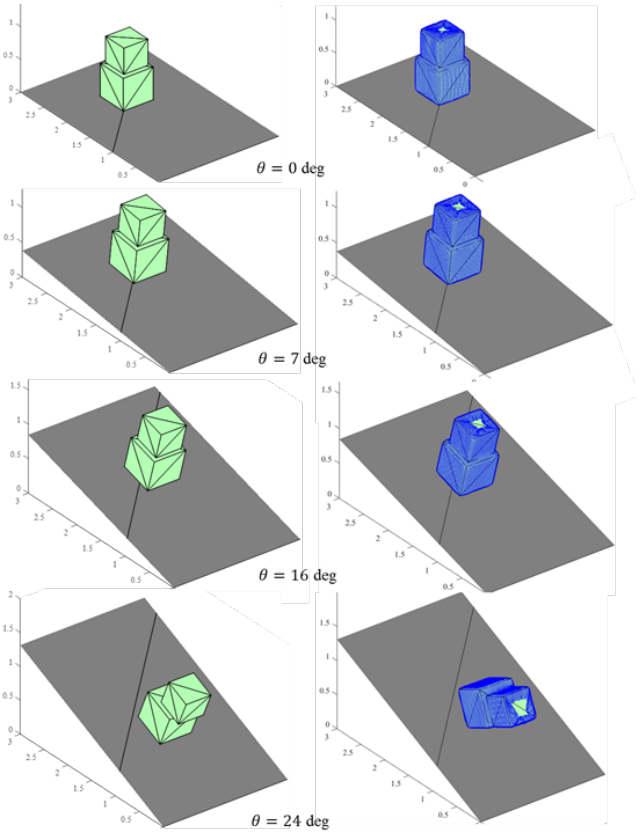


*Figure 7 Visualization of the simulated results*

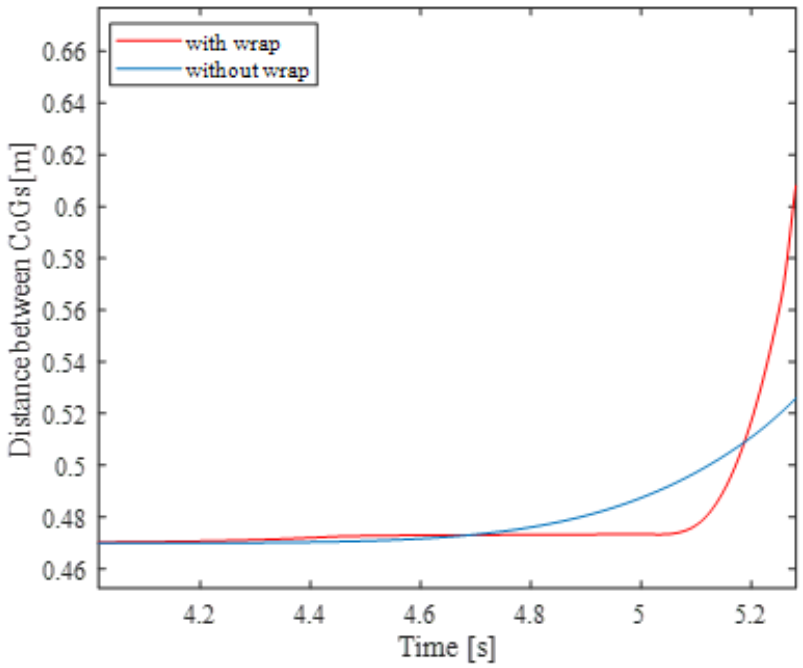


*Figure 8 Distance between the CoGs of the two bodies as slip measure*

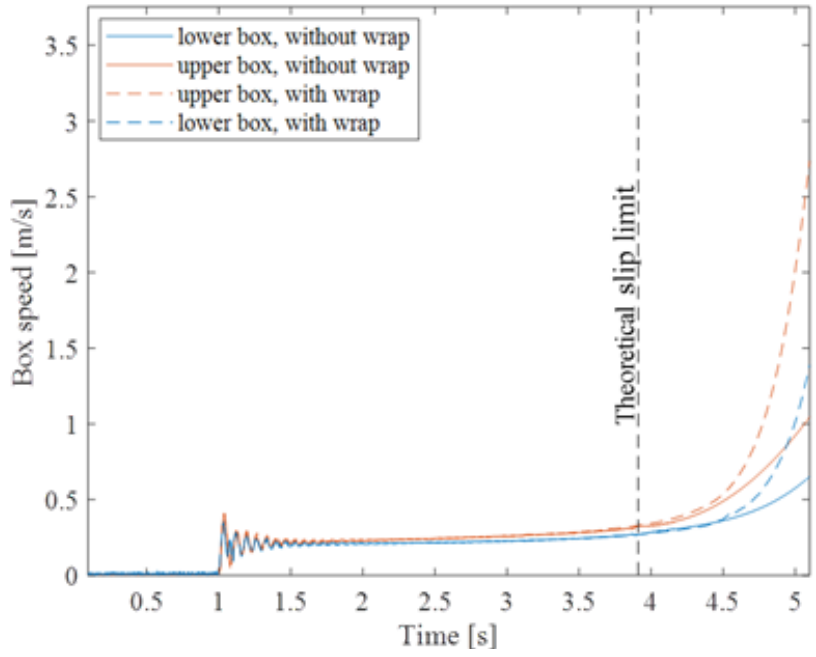


*Figure 9 Velocities of the two boxes during the first five seconds of simulated time*

## CONCLUSIONS

The developed model has for a simple test case proven capable of limiting slip and eventually tipping a stack of packed objects due to the dislocating of the CoG as slip occurs. Since these are the two main effects to be expected in the analysed benchmark case, the considered MBD framework seems to be a promising method for prediction of wrap film performance in packaging engineering. With experimentally determined wrap film material parameters and a failure criteria for rupture simulation, results obtained by simulation may serve as supporting tool for packaging testing.

If larger and more complex stacks of packed objects are to be simulated, it is likely that a hierarchical contact detection structure and a higher order solver allowing for a more coarse time discretization could increase the simulation speed.

## REFERENCES


[1] P. Singh, J. Singh, J. Antle and E. Topper, "Load Securement and Packaging Methods to Reduce Risk of Damage and Personal Injury for Cargo Freight in Truck, Container and Intermodal Shipment", in Journal of Applied Packaging Research, Vol. 6, No.1, 2014

[2] J, Singh, K. Saha and T. Sewell, "Evaluation of Stability of Unit Loads for Tilt and Shock Events During Distribution", in Journal of Applied Packaging Research, Vol. 9, No.3, 2017

[3] P.E. Nikravesh, Computer-aided analysis of mechanical systems, 1st ed.: Prentice Hall, 1989.

[4] S. Goyal, E.N. Pinson, F.W. Sinden, "Simulation of dynamics of interacting rigid bodies including friction Part I and II", in Engineering with Computers, vol. 10, 1994

[5] NH Ostergaard and S. Danjou, "On Numerical Simulation of the Dynamics of Bottles in Conveyor Systems", Journal of Applied Packaging Research, Vol. 9 (3), 2017

[6] S. Jevšnik, F. Kalaoğlu, S. Terliksiz and J. Purgaj, "Review of Computer Models for Fabric Simulation", Tekstilec, vol. 57 (4), 2014

[7] J.V. Bisha, "Correlation of the Elastic Properties of Stretch Film on Unit Load Containment", Doctoral thesis, Virginia Polytechnic institute and State University, 2012

[8] O. Etzmuss, J. Gross, and W. Strasser, "Deriving a Particle System from Continuum Mechanics for the Animation of Deformable Objects", IEEE Transactions on Visualization and Computer Graphics, Vol. 9, No. 4, 2003

[9] R. Rossi, M. Lazzari, R. Vitaliani and E. Onate, "Simulation of Light Weight Membrane Structures by Wrinkling Model", International Journal for Numerical Methods in Engineering, Vol. 62, 2005

[10] P. Contri and B.A. Schrefler, A Geometrically Nonlinear Finite Element Analysis of Wrinkled Membrane Surfaces by a no-Compression Material Model", Communications in Applied Numerical Methods, Vol. 4, 1988

[11] A.S. Knudsen, T. Stougaard and S.E. Sørensen, "Simulation and Optimization of Unloading Sequence" (In Danish, original title "Simulering og Optimering af afkastforløb", MSc Thesis, Aalborg University, 2007